Polym. Bull. (2017) 74:121–144
DOI 10.1007/s00289-016-1703-6

ORIGINAL PAPER

High-temperature study of radiation cross-linked ethylene–octene copolymers

Petr Svoboda[1]

Received: 20 November 2015 / Revised: 30 March 2016 / Accepted: 19 May 2016 /
Published online: 10 June 2016

Abstract Three ethylene–octene copolymers (EOC) with a wide range of octene content (17, 30, and 38 wt%) and with the same melt flow index of 1 g/10 min were cross-linked by e-beam radiation (in range 30–120 kGy). The testing methods comprised of rheology, a high-temperature creep test, an analysis of the gel content, and a dynamic mechanical analysis (DMA) test. It was discovered that copolymers with a high octene content attain a higher level of cross-linking density. Cross-linking influenced properties below T_m only marginally as seen from the DMA results. However, the properties above T_m were highly influenced as detected by high-temperature creep and rheology. Above T_m, without the presence of crystals, only the chemical bonds holding the amorphous chains together manifested a gradually decreasing creep at 150 °C with an increasing irradiation level. The loss factor (tanδ at 0.1 Hz) at 150 °C revealed a decreasing trend (or higher cross-linking level) with an increasing octene content. High-temperature results were supported by an increasing gel content with increasing octene content. Samples irradiated to 30 kGy dissolved completely in xylene but showed significantly changed rheological characteristics indicating only an increase in the molecular weight and branching. Analysis according to the Charlesby–Pinner equation revealed increased cross-linking to the scission ratio $G(X)/G(S)$ for EOCs with a higher octene content. While the q_0 value which relates to cross-linking changed only slightly, a significant decrease in the p_0 value which relates to chain scission was discovered.

Keywords Ethylene–octene copolymer · Electron beam irradiation · Cross-linking · Rheology · Creep

✉ Petr Svoboda
svoboda@ft.utb.cz

[1] Department of Polymer Engineering, Faculty of Technology, Tomas Bata University in Zlin, Vavreckova 275, 762 72 Zlin, Czech Republic

Introduction

The development of Dow's INSITE® metallocene catalysts led to the launch of many new polyolefin products which had previously been unattainable from the conventional Ziegler–Natta catalysis [1]. Copolymers of ethylene and alpha-olefins, e.g., linear low-density polyethylene (LLDPE), synthesized using the conventional multisite Ziegler–Natta catalysts are known to have broad molecular weight distributions (MWD) and also broad comonomer distributions [2]. This new class of copolymers has a narrow MWD, a very uniform narrow comonomer distribution and a controlled level of long chain branching (LCB) which leads to an unusually good processability (shear thinning). The incorporation of an alpha-olefin comonomer in the ethylene chains disrupts the chain regularity which then leads to a very special spot-like crystalline structure and smaller crystallinity. This unique crystalline structure then influences the mechanical properties. During the tensile test, the yield point is not present. In addition, the elastic behaviour is also greatly improved, which is manifested by a hugely reduced permanent set after repeated elongation to 100 % [2].

The unique microstructure of constrained geometry catalyst technology (CGCT) copolymers introduces an opportunity to study structure–property relationships solely as a function of one variable while keeping other variables constant. For example, Alamo et al. investigated the influence of comonomer types (butene, hexene, and octene) and molecular weight [3], Bensason et al. studied the influence of the comonomer content [4], and Wood-Adams et al. focused on the influence of LCB [5].

These copolymers have good tear resistance and a long shelf life which make them ideal packaging materials [6]. They may also be used as high-performance elastic fibers for apparel [7] (to replace Elastane), soft foams [8, 9], and in biomedical applications, including catheters and blood bags [6].

Commercially successful olefinic copolymers include ethylene–propylene, ethylene–butene, and ethylene–octene. Side groups differ only by the length or by the number of CH_2 groups (1, 2, or 6) that are attached to the ethylene main chain. Interestingly, a similar rubber product, ethylene–styrene copolymer [1, 10] was produced for several years and used, e.g., in the foaming industry; however, after several years, its production stopped due to its low profitability. In contrast, ethylene–octene copolymer (EOC) has found its place in high-volume production, and now, after more than 15 years, it is being produced and sold.

The above-mentioned disruption of the chain regularity leads not only to improved elastic properties, but at the same time to a decreased melting temperature (T_m) [3, 11, 12]. The "spot-like" crystals act as tie points for amorphous chains. However, at temperatures above T_m, the polymer starts to flow freely. This could be a serious problem for many articles made from these copolymers, since T_m for the most elastic articles is in the range of 45–55 °C [11]. Fortunately, this shortcoming can be overcome by cross-linking, as shown for Dow XLA™ elastic fiber [7]. Then, after the disappearance of physical cross-linking above T_m (melting of crystalline tie points), chemical cross-linking (covalent bonds) ensures the elastic recovery after stretching.

Commercially successful methods for cross-linking of saturated polyolefins include peroxide cross-linking at elevated temperatures (such as dicumyl peroxide) [8, 13, 14]; grafting by vinyltrimethoxy silane in the presence of peroxide followed by the addition of a catalyst and exposure to water or humidity at elevated temperatures [15–17] and finally cross-linking by gamma [18–20] or electron beam [21–23] radiation. All these cross-linking methods have advantages and disadvantages. Nevertheless, all of them are being used commercially.

In spite of the fact that some researchers have attempted to compare the cross-linking behaviour of these copolymers under radiation, regrettably they varied several parameters at the same time (e.g., octene content and also molecular weight) which have led to questionable conclusions. At present, there is no solid understanding of the effect of octene content on cross-linkability by irradiation. To get a scientifically sound conclusion, in this study, there was only one variable (octene content) while keeping all other parameters constant.

This paper focuses only on electron beam irradiation cross-linking in connection with ethylene–octene copolymers. More specifically, the influence of the octene content (or branching density) on cross-linkability with the help of the measurement of rheology and creep behaviour at 150 °C and cross-link density by the gel content after the extraction of the soluble portion of the non-cross-linked polymer chains was examined. The data were evaluated by the Charlesby–Pinner equation.

Experiment

Materials

Three different ethylene–octene copolymers with the trade name ENGAGE® were used; they were supplied by The Dow Chemical Company (Midland, Michigan, USA). The octene contents of these copolymers were 17, 30, and 38 wt%. For a better understanding, the abbreviations EOC-17, EOC-30, and EOC-38 were chosen according to the octene content in wt%. The detailed compositions and densities are listed in Table 1. The initial melt flow indexes (MFI) were purposely the same for all three copolymers, being 1.0 g/10 min at 190 °C.

Table 1 Composition and density of investigated ethylene–octene copolymers (EOC)

Abbreviation	Trade name	Octene (wt%)	Ethylene (wt%)	Octene (mol %)	Ethylene (mol %)	ET/OCT (molar ratio)	Density (g/cm^3)
EOC-17	ENGAGE 8540	17	83	4.87	95.13	19.5	0.908
EOC-30	ENGAGE 8003	30	70	9.68	90.32	9.3	0.885
EOC-38	ENGAGE 8100	38	62	13.29	86.71	6.5	0.870

MFI at 190 °C was for all samples 1.0 g/10 min

Low-density polyethylene (LDPE) which has been used for a comparison of some properties was Bralene RB 2-62, manufactured by Slovnaft Petrochemicals, Bratislava, Slovak Republic. MFI and the density of Bralene RB 2-62 were 2 g 10 min^{-1} and 0.918 g cm^{-3}, respectively.

Compression moulding of the sheets

Sheets with a thickness of 0.5 mm (stainless steel frame size was 12 × 6 cm) were prepared by compression moulding. Pellets were pre-heated at 130 °C under minimal pressure for 5 min and compressed at 10 MPa for 3 min in a laboratory press and then quenched in another cold press under pressure.

Electron beam irradiation

Electron irradiation was performed in normal air at room temperature in BGS Beta-Gamma-Service GmbH, Germany. The temperature was controlled not to exceed 50 °C. The source of radiation was toroid electron accelerator Rhodotron (10 MeV, 200 kW). The irradiation was carried out in a tunnel on a continuously moving conveyer with the irradiation dosage ranging from 30 to 120 kGy in steps of 30 kGy per pass. Samples were arranged in one layer sealed between PET sheets. Other important parameters were: 10 mA, conveyer belt speed 3 m/min, distance from scanner to sample 78 cm, and irradiation time 2 s.

Dynamic mechanical analysis (DMA)

Dynamic mechanical analysis was carried out in an IT Keisoku-seigyo (DVA-200S) machine (Osaka, Japan). Specimens were tested in the dynamic tensile mode with a frequency of 10 Hz and a strain of 0.1 % from −100 to +200 °C with a heating rate of 5 °C min^{-1} and a grip-to-grip distance of 13.0 mm. Sample dimensions were 40 × 5 × 0.5 mm.

Rheology

Advanced Rheometric Expansion System ARES 2000 (Rheometric Scientific, Inc., Piscataway, NJ, USA) equipped with 25 mm parallel plates geometry was used to determine storage modulus G′, loss modulus G'', and complex viscosity η^* in the frequency range 0.1–100 rad s^{-1} at constant temperature (150 °C) and strain (1 %). The loss factor was calculated as $\tan\delta = G''/G'$.

High-temperature creep test

Tensile samples were cut out of the cross-linked sheets and were used for the tensile creep experiments according to ISO 899. Creep testing was carried out in a Memmert UFE 400 oven with digital temperature control. Creep was recorded through the glass window using a SONY SLT-A33 camera, capable of HD 1920 × 1080 video (25 frames/s). This video was later analysed at regular time

intervals. The effects of octene content, MFI, and the radiation dose on the creep behaviour of e-beam cross-linked EOC were studied at a fixed stress level of 0.1 MPa and 150 °C.

Gel content

The gel contents of the e-beam cross-linked EOC and LDPE samples were determined by an evaluation of the content of insoluble fraction of cross-linked material after solvent extraction according to ASTM D2765-01. About 0.3 g of cross-linked sample was wrapped in a 120 mesh stainless steel cage and extracted in refluxing xylene containing 1 wt% of antioxidant (Irganox 1010) for 6 h. The sample was then dried in a vacuum at 55 °C and weighed. The gel content was calculated as a ratio of the final weight to the initial weight of the sample multiplied by one hundred. Three samples were always averaged.

Size-exclusion chromatography

The molecular weight measurements were performed at 160 °C on a Polymer Laboratories PL 220 high-temperature chromatograph (Polymer Laboratories, Varian Inc., Church Stretton, Shropshire, England) equipped with three 300 mm × 7.5 mm PLgel Olexis columns and a differential refractive index detector. 1,2,4-trichlorobenzene (TCB) was used as an eluent, stabilised with butylhydroxytoluene (BHT) (Ciba, Basel, Switzerland) as an antioxidant. A mobile phase flow rate of 1 mL min^{-1} was used, and 200 μL was injected in all the cases. All samples were prepared to a concentration of 0.5 mg mL^{-1} in TCB. Narrowly distributed polyethylene standards (Polymer Standards Service GmbH, Mainz, Germany) were used for calibration purposes.

Theoretical background

When radiation from a γ-ray, electron beam, or X-ray source interacts with a polymer material, its energy is absorbed by the polymer material and active species, such as radicals are produced, thereby initiating various chemical reactions. The fundamental processes that are the results of these reactions include [24]:

- Cross-linking, where polymer chains are joined and a network is formed.
- Chain scission, where the molecular weight of the polymer is reduced through chain scission.
- Oxidation, where the polymer molecules react with oxygen via peroxide radicals (oxidation and chain scission often occurs simultaneously).
- Long-chain branching, where polymer chains are joined, but a three-dimensional network is not yet formed.
- Grafting, where a new monomer is polymerized and grafted onto the base polymer chain.

Different polymers have different responses to radiation, especially when it comes to cross-linking vs. chain scission. A parameter called the G value is widely used by radiation chemists to quantify the chemical yield resulting from the radiation. The G value is defined as the chemical yield of radiation in a number of molecules reacted per 100 eV of absorbed energy. Materials with $G(S)$:$G(X)$ ratios <1.00 are favoured for cross-linking. Materials with $G(S)$:$G(X)$ ratios >1.00 tend to undergo degradation more. Materials, whose $G(X)$ and $G(S)$ values of both are low, are more resistant toward radiation. The different responses to radiation for different polymers are intrinsically related to the chemical structures of the polymers.

Cross-linking and chain scission are two competing processes that always co-exist under radiation. The overall effect depends on which of the two is predominant at a certain time. Whenever $G(X)$ is larger than $G(S)$, the overall result is cross-linking, and whenever $G(S)$ is larger than $G(X)$, the overall result is degradation. It should also be kept in mind that for a given polymer, both $G(X)$ and $G(S)$ change with radiation conditions, such as the absorbed dose and the temperature. For the relationship with the radiation dose, both $G(X)$ and $G(S)$ increase with the increase in the dose. However, $G(S)$ for a polymer generally increases more than $G(X)$ does with an increasing dose.

The different reactions that radiation incurs on a polymer bring about different effects on the physical properties of the polymer. Cross-linking normally enhances the mechanical properties and thermal stability of the polymer while reducing the melt flow and increasing the viscosity of polymer solution. Chain scission, on the contrary, deteriorates the mechanical integrity and thermal resistance. It increases the melt flow and decreases the viscosity of polymer solution. Oxidation may give rise to discolouration and brittleness and introduces carbonyl-containing functional groups to the polymer. Long-chain branching brings the modification of rheology and, hence, the processability of the polymer.

Estimation of G values of cross-linking by the Charlesby-Pinner method

In 1959, Charlesby and Pinner published research results concerning the solubility of irradiated polyethylene. They analysed the data with the help of the following equation [25]:

$$s + \sqrt{s} = \frac{p_0}{q_0} + \frac{1}{q_0 u_1 r} \tag{1}$$

where s is the sol fraction ($s + g = 1$), g is the gel fraction, r is the radiation dose, p_0 is the fracture density per unit dose, q_0 is the density of cross-linked units per unit dose, and u_1 is the number-average degree of polymerization.

These days, the same equation is frequently expressed as [26]:

$$s + \sqrt{s} = \frac{p_0}{q_0} + \frac{1}{q_0 P_n D} \tag{2}$$

where P_n is the initial number-averaged degree of polymerization, and D is the absorbed radiation dose in kGy [27].

Many radiation-induced chemical changes are measured quantitatively in terms of a G value, this being the number of such changes produced per 100 eV absorbed in the system [25]. G values for cross-linking and chain scission are expressed as $G(X)$ and $G(S)$, respectively. Cross-linking and chain scission are two competing processes that always co-exist under radiation. The overall effect depends on which of the two is pre-dominant at a certain time. Whenever $G(X)$ is larger than $G(S)$, the overall result is cross-linking, and whenever $G(S)$ is larger than $G(X)$, the overall result is degradation. Charlesby and Pinner equation containing G values is expressed as [24]:

$$s + \sqrt{s} = \frac{G(S)}{2G(X)} + \frac{4.82 \times 10^6}{G(X)M_nD} \tag{3}$$

where M_n is the number-averaged molecular weight.

Turgis et al. used a modified version of this equation for copolymers AB [28]:

$$s + \sqrt{s} = \frac{G(S)}{2G(X)} + \frac{9.65 \cdot 10^6 \cdot m_A}{G(X) \cdot D \cdot M_w \cdot [x_B \cdot m_B + (1 - x_B) \cdot m_A]} \tag{4}$$

where m_A and m_B are molecular weights of comonomer units A and B, respectively. x_B is the molar fraction of comonomer B.

Results and discussion

In general, rubber studies have involved only the complex dynamic shear modulus, G^*, rather than its two components, G', the storage or elastic shear modulus, and G'', the loss or viscous modulus [29],

$$G^* = G' + iG'' \tag{5}$$

The cross-linking system can be assumed to be an ideal rubber from the gel point to somewhere near the rubber to glass transition. From the rubber elasticity theory, we can relate the modulus determined at small deformations directly to the cross-link density, X [29]:

$$|G^*| = \mathrm{RTX} \tag{6}$$

In general, $G'' \ll G'$ after the gel point. Thus, one can focus on the development of only G' value [29].

Initially, the rheology at 150 °C was measured for all three ethylene–octene copolymers exposed to various levels of irradiation. The three EOC samples before irradiation had slightly different modulus G' values. Therefore, rather than plotting the absolute G' values, it seemed more appropriate to show the relative G' increase after irradiation. This is shown in Fig. 1a. For the EOC-17, the relative increase of G' was in the range 15–42. For the EOC-30, the relative increase of G' was higher (in the range 34–101). The highest relative increase of G' was found for EOC-38 (in the range 53–126).

For the irradiations 60, 90, and 120 kGy, the G' values for EOC-17 were 27.9, 32.0, and 43.4 kPa, and for EOC-38, they were 29.7, 38.9, and 53.7 kPa. These increases in G' have slope values 259.5 and 400.2, for EOC-17 and EOC-38, respectively. The slope value for EOC-38 is about 54 % higher than that for EOC-17. From the steeper increase in G' for EOC-38, one can assume a steeper increase in cross-link density X as a function of irradiation.

Figure 1b shows the influence of the octene content on relative G' increase for various radiation levels (30, 60, 90, and 120 kGy). This measurement suggests that an EOC with a higher octene content cross-links more efficiently than the one with a lower octene content. A rheology measurement was analysed further with the focus on a loss factor tanδ (tan$\delta = G''/G'$) which is the richest source of information regarding the molecular structure. In general, it is accepted that lower tanδ relates to better cross-linking. The tanδ results from ARES rheology (at 150 °C) are shown in Fig. 2.

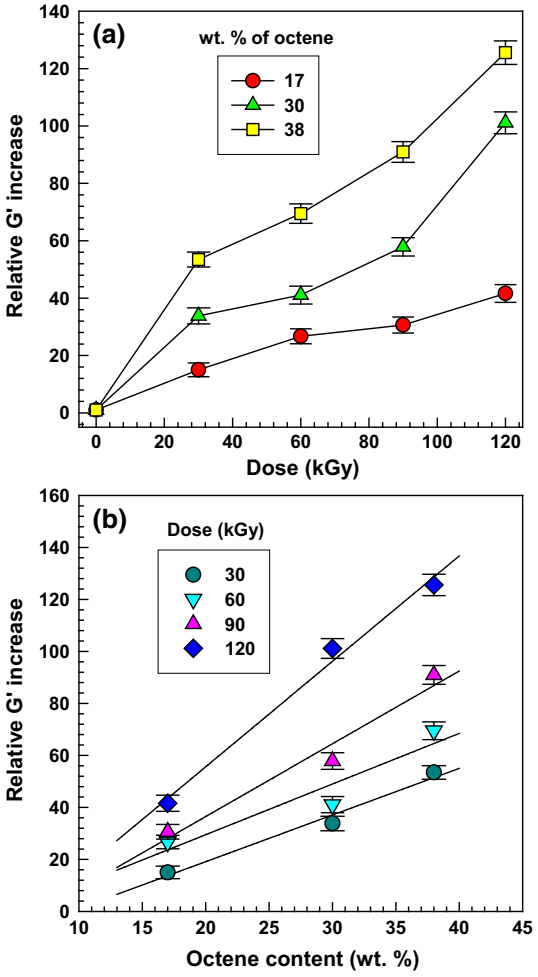

Fig. 1 Relative G' increase from rheology measurement on ARES Rheometer at 150 °C and 0.1 rad/s

First, Fig. 2a shows tanδ as a function of frequency for all three EOCs before cross-linking. Note that the tanδ values at 0.1 rad/s are in the range of 2.7–5.5. After irradiation to 120 kGy level, the tanδ values at 0.1 rad/s dropped in all EOCs to 0.17–0.35 range. At a higher frequency, the dangling chain behaves like the cross-linked one and the entanglement behaves like cross-linking. At a lower frequency, the chain shows characteristic viscoelastic behaviour like the linear chain. Therefore, the lower frequency (0.1 rad/s) was chosen to illustrate the differences in cross-linkability, as shown in Fig. 2c, d.

The influence of radiation dose on tanδ decrease is best visible in Fig. 2c. Note that tanδ axis is in a logarithmic scale; that large was the decrease caused by radiation cross-linking. The influence of octene content is best visible in Fig. 2d. EOCs with a high octene content exhibit lower values of tanδ which corresponds to better cross-linking.

The rheology measurements rendered not only the G' and tanδ values (shown in Figs. 1, 2) but also the viscosity values. Viscosity is very sensitive to changes in chain length and is routinely used to characterise polymer molecular weight. Power

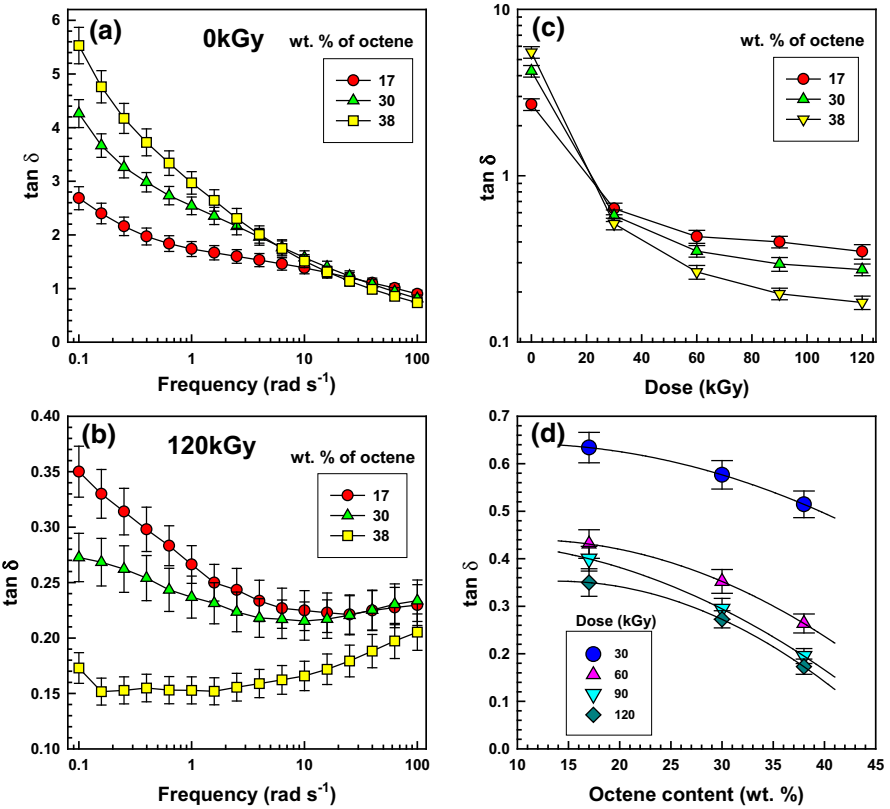

Fig. 2 Rheology results from ARES Rheometer at 150 °C. **a**, **b** as a function of frequency, **c** and **d** for frequency 0.1 rad/s

law can be used to describe the relation of viscosity and molecular weight for entangled polymers [30]:

$$\eta = \mathrm{KM}^{3.4} \tag{7}$$

From the increase of viscosity caused by radiation, one can estimate the increase in molecular weight. Since radiation dose 60–120 kGy led to insoluble gel, only the 30 kGy level could be used for this calculation. The following equation was used to estimate the molecular weight increase:

$$\frac{M_{30\mathrm{kGy}}}{M_{0\mathrm{kGy}}} = 10^{\frac{\log\left(\eta_{30\mathrm{kGy}}/\eta_{0\mathrm{kGy}}\right)}{3.4}} \tag{8}$$

The increase in viscosity $\left(\eta_{30\mathrm{kGy}}/\eta_{0\mathrm{kGy}}\right)$ due to the irradiation 30 kGy for EOC-17, 30, and 38 was about 6.1, 8.8, and 10.7, respectively. Consequently, the calculated molecular weight increase $\left(M_{30\mathrm{kGy}}/M_{0\mathrm{kGy}}\right)$ for EOC-17, 30, and 38 was about 1.7, 1.9, and 2.0, respectively. Copolymers with a higher octene content manifested the higher increase in viscosity caused by 30 kGy irradiation which can be interpreted by a higher increase in the molecular weight.

Visibility of the of cross-linking level is better at elevated temperatures (above melting point) when the molecules are only held together by chemical covalent bonds and not by physical cross-linking (when the crystals hold together the amorphous chains). Therefore, the samples were tested for creep behaviour at 150 °C. Figure 3a shows the creep development over time. Within 100 s, the creep values were small and similar for all three EOCs. In the range 100–1000 s, the creep curves grew substantially and differently for different EOC samples. The influence of EOC content is best visible in Fig. 3b. For all listed times [log(time/s) values], the creep values are smaller for EOCs with a higher octene content. High-temperature creep was also evaluated quantitatively as a slope of the line in the time range 4–25 min. The slope values for EOC-17, 30, and 38 were 35.3, 23.3, and 14.1, respectively. There is a huge influence of the octene content on a slope of the creep compliance. EOC with higher octene content exhibits significantly lower slope values.

The gel content study (see Fig. 4) reveals the amount of an insoluble cross-linked portion of polymer chains. After 6 h boiling in 138 °C xylene in a cage formed from stainless wire net with a gap between the wires of 0.2 mm, all the soluble molecules dissolve into the xylene. In the case of original samples without radiation exposure (see Fig. 4a), all of them completely (100 %) dissolved in xylene. Interestingly, also all 30 kGy radiated samples completely dissolved. If we looked only at these results, one could conclude that 30 kGy irradiation did not cause any visible change. However, we have to look also at the results from other analyses (previously shown in Figs. 2 and 3 where even 30 kGy caused a considerable increase in G' and a decrease in $\tan\delta$. One conclusion is that 30 kGy causes only an increase in molecular weight and branching, but the full three-dimensional network has not been formed yet. A radiation dose of 60 kGy had already caused the generation of

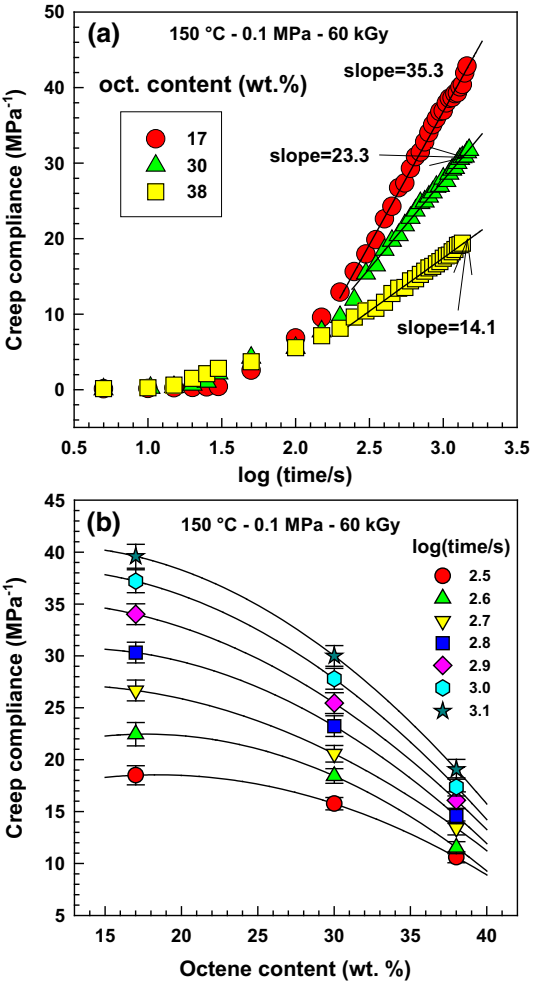

Fig. 3 Creep behaviour at 150 °C at stress 0.1 MPa for samples radiated to 60 kGy level

an insoluble 3D network ranging according to the sample from 52 to 74 %. In the radiation range 60–120 kGy, the gel content is increasing only moderately (compared to a large jump in the range 30–60 kGy). Figure 4b shows the influence of octene content on the gel content for radiation doses 60, 90, and 120 kGy. In this gel content study, we also tested a low-density polyethylene (LDPE) to which the 0 octene content was assigned. Interestingly, the LDPE fits almost perfectly to the linear regression lines, as shown in Fig. 4b. With increasing octene content, the gel content also increased.

The solubility of the three ethylene–octene copolymers and LDPE was initially analysed with the help of Eq. (2) (see Fig. 4c). This led to intercept values p_0/q_0 (scission to cross-linking ratio) and slope values being $1/q_0P_n$. More detailed analysis shown in "Appendix 2" then led also to other values: q_0, p_0, $G(X)/G(S)$, $G(X)$, and $G(S)$. Comparison of these values is shown in Fig. 5.

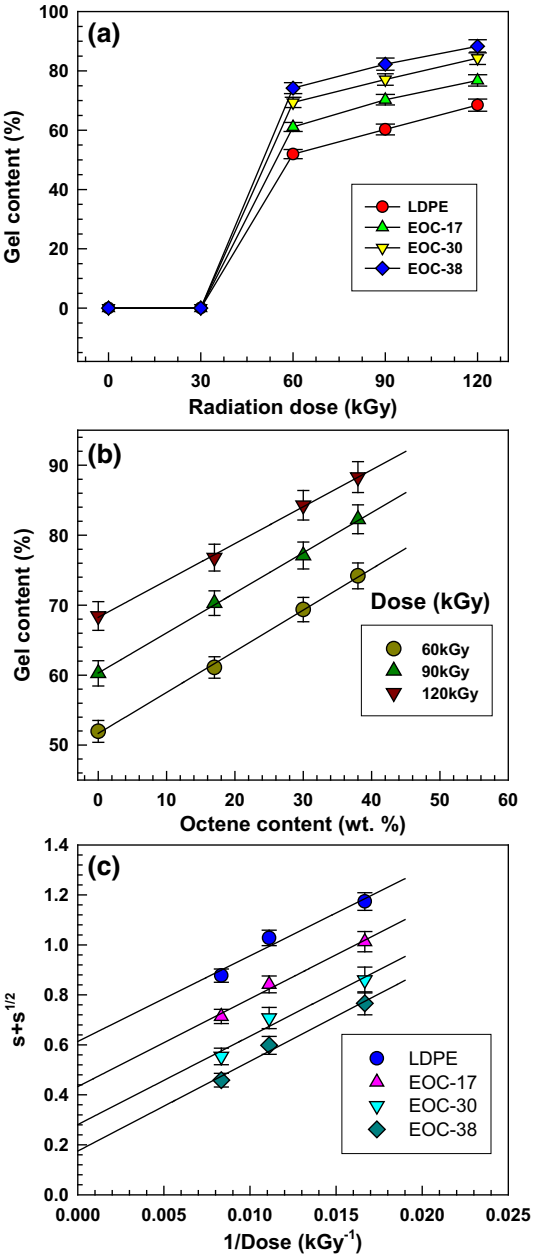

Fig. 4 **a**, **b** Gel content results for three radiation cross-linked ethylene–octene copolymers plus LDPE. **c** Charlesby–Pinner analysis

The density of cross-linked units per unit dose (q_0) is quite similar for all samples. However, the fracture density per unit dose (p_0) is quite different; it is considerably lower for EOCs with a higher octene content. Reduced scission then leads to a substantially higher cross-linking to a scission ratio $G(X)/G(S)$ for the

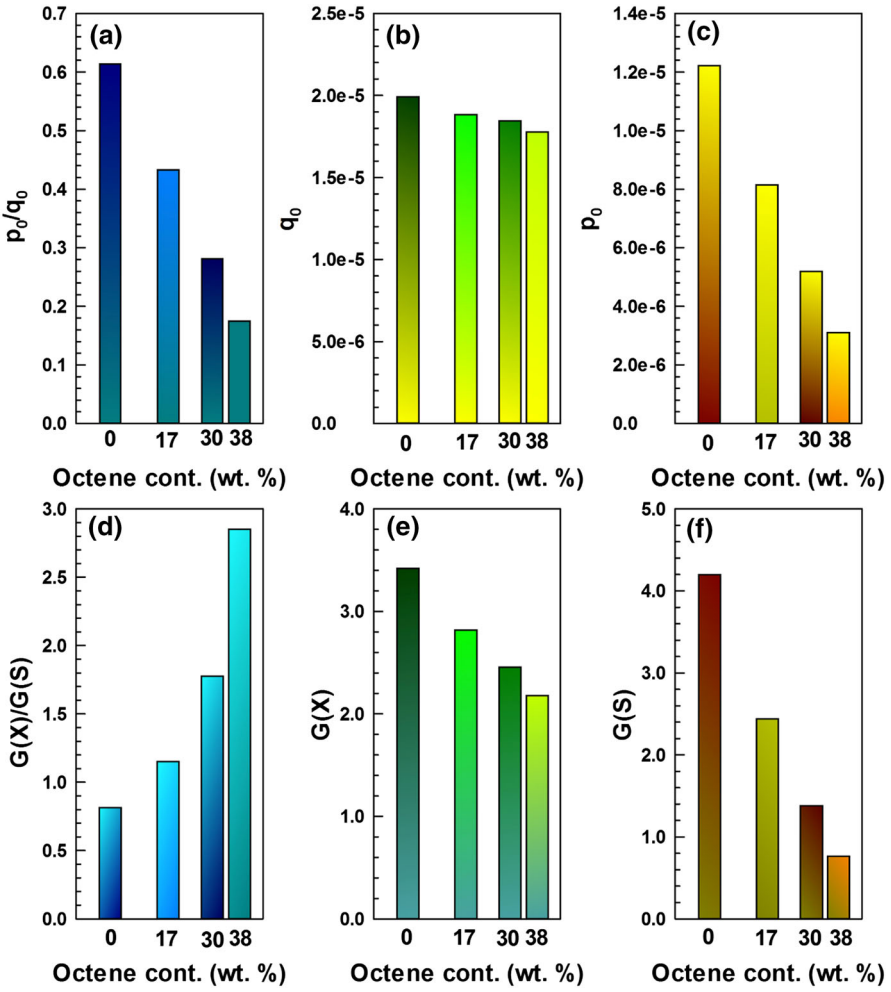

Fig. 5 Charlesby–Pinner analysis—results: **a** p_0/q_0, **b** q_0, **c** p_0, **d** $G(X)/G(S)$, **e** $G(X)$, **f** $G(S)$

copolymers with a higher octene content. With a higher content of octene short branches, the probability of a radical formation on a short branch increases, and consequently, the main chain is attacked to a lesser extent. The mobility of the short branch is much higher, compared to the one on the main chain, so that the radicals on octene have a higher probability for recombination with other free radicals which leads to cross-linking. The situation is schematically shown in Fig. 7. A free radical can lead to cross-linking or scission. A copolymer with a higher octene content has more short-chain branches and thus the probability of radical formation on a branch is higher (options c and d). While scission on a main chain (options a and b) leads to a decreased molecular weight, scission on an octene short branch influences the molecular weight only minimally.

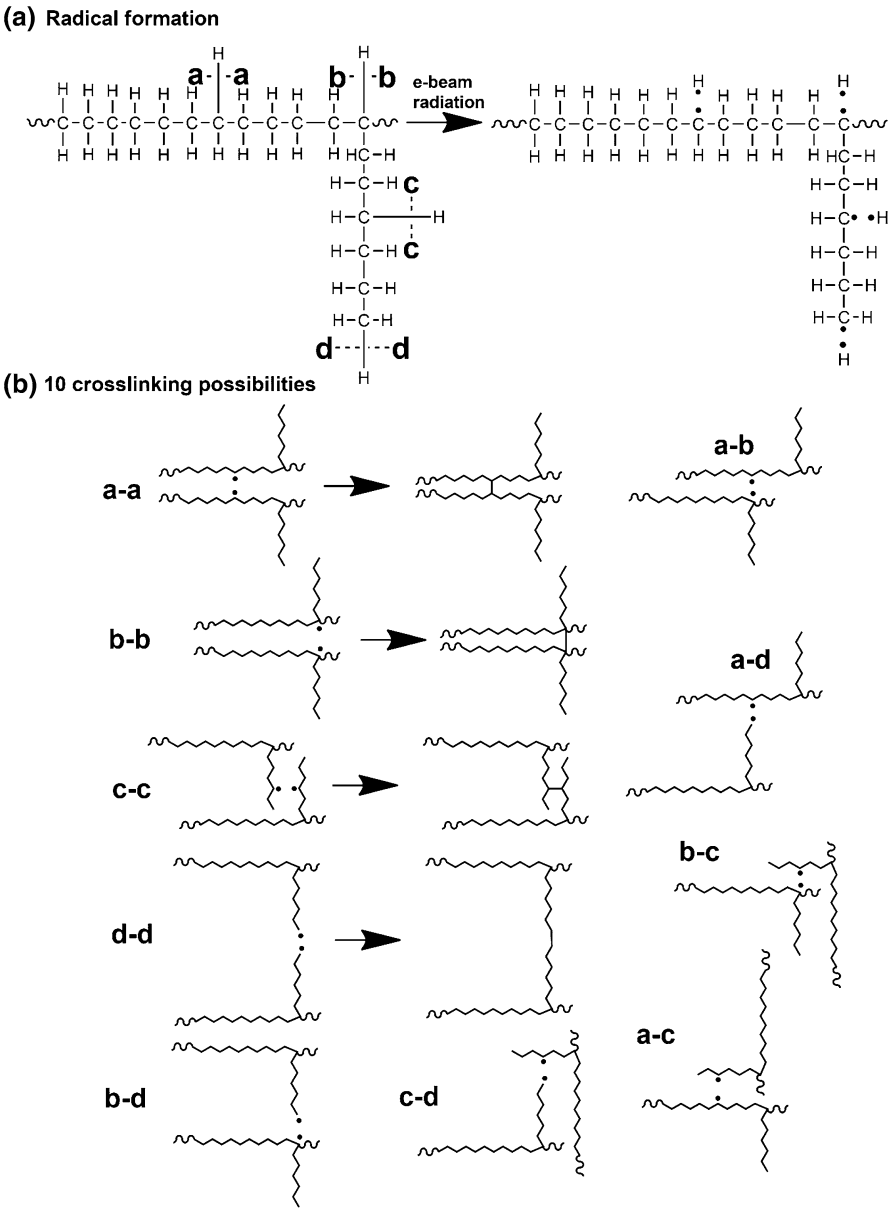

Fig. 6 Schematic representation of **a** radical formation and **b** ten cross-linking possibilities

Another significant fact is that a copolymer with a higher octene content includes a higher number of tertiary carbon atoms. After being exposed to e-beam radiation, the hydrogen atoms are extracted from carbon atoms. The radical on a tertiary carbon atom can be created more easily, even though the radicals on the main chain

or on an octene branch are formed as well (LDPE was also cross-linked, however, to a lower extent). The polymer radicals can then form a cross-link by a recombination with another polymer radical or they can extract a hydrogen atom from the neighbouring chain. Cross-linking options in Fig. 6b–b, b–d, a–b, and b–c play an important role during electron beam cross-linking of ethylene–octene copolymers. As it was shown, LDPE also cross-links (a–a option) but to a lesser extent. Solubility results agreed well with previously shown rheology and creep results.

The presented results are in good accord with other researchers [8, 9, 31, 32]. For instance, Vachon et al. extensively examined the foaming behaviour of gamma-irradiated ethylene–octene copolymers. Cross-linking not only stabilises bubble growth during expansion but also enhances the resistance of cellular material to thermal collapse. While insufficient cross-linking may lead to collapse, excessive cross-linking may restrict the foam expansion. The EOCs had the same melt flow index (MFI = 1 g/10 min) while increasing octene content EOC-30 (Engage 8003) and EOC-38 (Engage 8100). After irradiation to 50 kGy in the air, the copolymer with a higher octene content (EOC-38) demonstrated 80 % gel content, while the one with the lower octene content (EOC-30) had only 68 % gel content. After irradiation to 100 kGy in a vacuum, the values were 88 and 85 % for EOC-38 and EOC-30, respectively [9].

Liu et al. investigated UV photodegradation of polyethylene compared to ethylene–octene copolymers with an increasing octene content 20, 30, and 38 wt%. After 200 h of UV exposure, the values of gel content for LDPE, EOC-20, EOC-30, and EOC-38 were 18, 22, 31, and 41 %, respectively. They evaluated the gel content also as a function of time. While LDPE exhibited a steady increase of gel, after 200, 300, 400, and 600 h, the values of gel content were 18, 31, 33, and 36 %, the EOC-38 had an initial sharp increase followed by a steady decrease, and the values were 41, 30, 18, and 7 %. These results indicate a much higher reactivity of EOC containing a tertiary carbon atom which initially leads to a higher level of cross-linking but later leads to a chain scission [32].

Sirisinha et al. investigated a silane cross-linked EOC (Engage 8003) in comparison with LDPE. These products are commonly used for a number of industrial applications, including wire and cable coating, hot-water piping insulation, and heat-shrinkable products. They found out that LDPE had a lower cross-linking rate and a lower gel content compared to EOC. The values of gel content after various water immersion times of 120, 360, and 600 h were for LDPE 52, 66, and 68 %, and for EOC-30, they were 77, 82, and 85 % [31].

Abe et al. conducted research concerning the foaming behaviour of ethylene–1-hexene copolymers that can be used as thermal insulation, floatation, automotive trim, and sports goods. He focused on two ethylene–1-hexene copolymers; LL1 had 25 branches, and LL2 had 7 branches per 1000 backbone carbon atoms with the same molecular weight of $M_n = 4.6 \times 10^4$ g/mol. The foams were produced directly by a moulding with 0.1–0.9 wt% of dicumylperoxide (DCP) and 8 phr of a blowing agent. The copolymer with the higher branching density (LL1) rendered a foam with a higher gel content, higher storage modulus G', and a lower tanδ. For example, for the peroxide concentrations 0.3, 0.5, 0.7, and 0.9 %, the values of gel content were 70, 88, 91, and 94 % for LL2 with 7 branches, and 73, 94, 96, and

98 % for LL1 with 25 branches per 1000 backbone carbon atoms. For peroxide concentrations 0.3 and 0.9 %, the storage modulus G' values (at 190 °C) were 273 and 431 kPa for LL2 with 7 branches and 319 and 611 kPa for LL1 with 25 branches per 1000 backbone carbon atoms. For peroxide concentrations 0.3 and 0.9 %, the loss factor tanδ values (at 190 °C) were 0.161 and 0.084 for LL2 with 7 branches and 0.122 and 0.053 for LL1 with 25 branches per 1000 backbone carbon atoms [8].

Nicolas et al. studied the cross-linking behaviour of EOCs by e-beam and peroxide. They selected Engage 8411 (with MFI = 18 g/10 min and 33 wt% of octene) and Engage 8400 (with MFI = 30 g/10 min and 40 wt% of octene). They concluded that increasing comonomer content reduces the cross-linking efficiency, because, for example, after irradiation with 200 kGy, the EOC with 40 wt% of octene had only 58 % gel content and EOC with 33 wt% of octene had 68 % gel content [14]. The problem with their conclusion is in the fact that these two copolymers have very different initial molecular weights. Recently, we have discovered the enormous influence of the initial molecular weight on cross-linking. For example, EOCs with approximately the same octene content (35, 38, and 39 wt%) with the initial melt flow index being 3, 1, and 0.5 g/10 min (molecular weight M_w being about 93,000, 129,000, and 167,000 g/mol), respectively, exhibited increasing gel content after e-beam irradiation to 120 kGy. The gel content values were 80, 88, and 91 %, respectively. The EOC with the lowest MFI (or the highest molecular weight) showed the highest gel content (91 %). Even more pronounced difference was visible at 60 kGy, gel content values being 56, 74, and 78 %, respectively.

In the past, we have investigated the cross-linking of EOCs by peroxide at higher temperatures (150–200 °C) [33]. This research led to the conclusion that the EOCs with lower octene content cross-linked better. The difference can be explained by a different cross-linking mechanism in the solid state (with the presence of a crystalline phase) versus cross-linking in the melting phase (with only an amorphous phase and much higher mobility). It is possible that a higher reactivity of tertiary carbon atoms at elevated temperatures initially leads to higher cross-linking, but later, the chain scission destroys the formed network, as reported by Liu et al. [32].

Conclusions

The three different analyses (rheology, high-temperature creep, and gel content) independently confirm that ethylene–octene copolymers with higher octene content cross-link better than ones with low octene content.

Rheology at 150 °C highlighted the huge differences in cross-linked polymers, especially in the 0–60 kGy range and at small frequencies (0.1–1 Hz). After irradiation, tanδ decreases significantly with increasing octene content which corresponds to a better elasticity (or a higher level of cross-linking).

The high-temperature creep test showed again how a decreasing trend in creep (or better resistance to flow) with an increasing octene content confirms a higher level of cross-linking.

Analysis of insoluble gel content illustrates how higher values for EOCs with higher octene content confirm a higher level of cross-linking. Analysis according to the Charlesby–Pinner equation manifests enlarged cross-linking to the scission $G(X)/G(S)$ ratio for higher octene EOCs. Compelling is a substantial decrease in $G(S)$ parameters. This was interpreted by scission on an octene short-chain branch which does not cause the main chain scission (and, e.g., EOC-38 has more octene short branches than EOC-30 and still more than EOC-17). Furthermore, in EOC-38, the amount of tertiary carbon atoms with higher reactivity is greater.

Acknowledgments This work has been supported by the Internal Grant Agency of the Tomas Bata University in Zlin number IGA/FT/2016/009.

Appendix 1

Furthermore, the irradiated samples were also analysed by dynamic mechanical analysis (DMA). The results are shown in Figs. 7 and 8. The curves of storage modules for the three samples (see Fig. 7) are quite different. Initially, there is a glassy plateau down to about −50 °C which is very similar for all three samples. Then, from −50 °C, the values of storage modulus differ to a large extent. EOC-17 decreases with increasing temperatures the least. On the contrary, EOC-38 decreases with increasing temperature quite significantly. EOC-30 is placed in between. The first drop is connected with glass transition temperature (T_g), and the second drop is connected with melting temperature (T_m). Figure 7b shows the tanδ dependence on temperature when T_g can be easily read as a peak position. The tanδ peak increases and moves towards a lower temperature with an increasing octene content.

The presented DMA results of the cross-linked samples resemble results for pure ethylene–octene copolymers presented by Bensason et al. [4]. He discovered that β and α relaxations strongly depend on octene content, while γ relaxation was the least sensitive to comonomer content. With increasing comonomer content, the α relaxation shifts to lower temperatures and starts to overlap with increasingly intense β relaxation. β relaxation (the largest peak is approximately −40 °C) is being interpreted as the glass transition temperature (T_g).

Figure 7a, b are shown for samples irradiated to 120 kGy. Is there any influence of the radiation on T_g? The answer to this question can be seen in Fig. 8a.

There is a clear trend in a T_g decrease with increasing octene content. However, as for the different levels of radiation, the T_g values are almost unchanged. Clearly, the radiation cross-linking influences the polymer behaviour more significantly above the melting point, at elevated temperatures as presented above. At lower temperatures, almost no difference was observed.

In contrast to almost no effect of radiation on T_g, there is a significant decrease in a storage modulus with increasing octene content; the polymer is becoming softer and rubbery (see Fig. 8b). A slightly smaller difference was observed at lower temperatures (−40 and −50 °C), but quite a large difference at higher temperatures

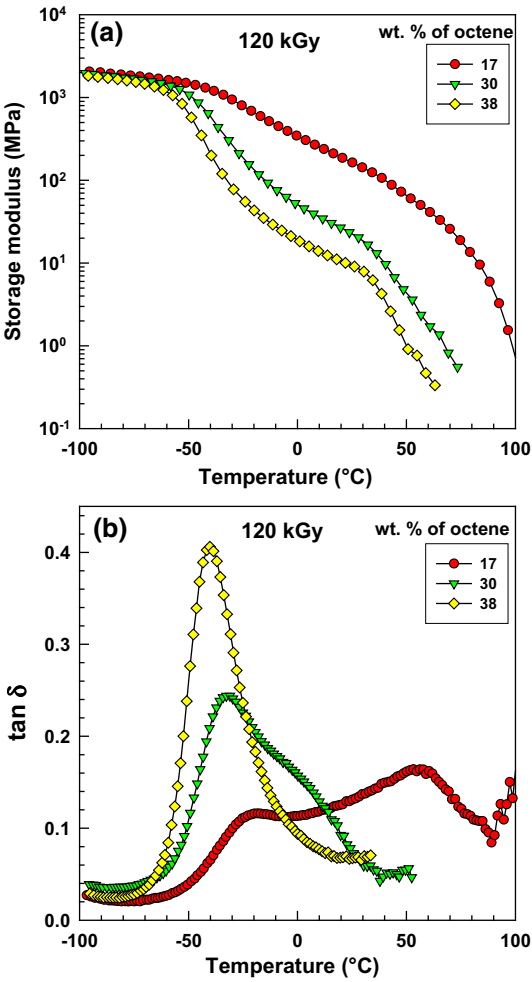

Fig. 7 DMA analysis results

(−20, 0, 20, 40 °C). Note that the storage modulus axis is in logarithmic scale, so the softness of the EOC samples is to a large extent different.

Tensile strength and modulus of semicrystalline polymers at temperatures below melting point come mainly from lamellar crystals that hold together amorphous chains. Tie molecules connect different crystals through amorphous phase. It is called "physical cross-linking". Such system has cohesive energy density (CED) of several orders of magnitude higher than lightly cross-linked semicrystalline polymer above melting point. Therefore, the effect of radiation on solid-state mechanical properties is very small. The cohesive energy represents the total attractive forces within a condensed state resulting from intermolecular interactions and consists of electrostatic interactions, van der Waals interactions, and hydrogen bonds interactions [34]. It is equivalent to the amount of energy required to separate the constituent atoms/molecules to an infinite distance, where it approaches zero

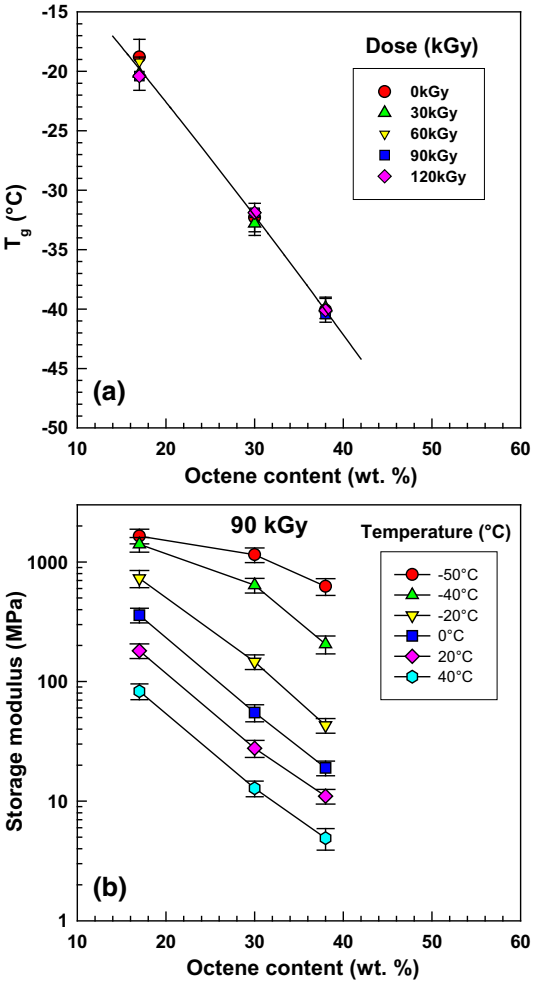

Fig. 8 DMA analysis results—continuation

potential energy. Cohesive energy density (CED) refers to the energy required to vaporise a mole of liquid per unit volume and is mathematically defined by:

$$\mathrm{CED} = \frac{\Delta E_V}{V_m} = \frac{\Delta H_v - RT}{V_m} \tag{9}$$

where ΔE_V = internal energy change of vaporisation, ΔH_v = enthalpy of vaporisation, V_m = molar volume of the liquid at the temperature of vaporisation, R = gas constant, and T = absolute temperature.

At higher temperatures (e.g., at 150 °C), above the melting point of EOC, there are no crystals to hold the amorphous chains together. The strength of the material comes only from the chemical bonds between chains (chemical cross-linking), and therefore, such high-temperature tests are very sensitive to the level of cross-linking.

Appendix 2

Example of calculation for EOC-38.
38 wt% of octene, $M_n = 61{,}469$ g/mol

$$\text{ethylene} = -CH_2 - CH_2-,\ M_{ET} = 2 \cdot C + 4 \cdot H = 2 \cdot 12.011 + 4 \cdot 1.008 = 28.054 \text{ g/mol}$$

$$\text{octene} = C_8H_{16},\ M_{OCT} = 8 \cdot C + 16 \cdot H = 8 \cdot 12.011 + 16 \cdot 1.008 = 112.216 \text{ g/mol}$$

$$\text{wt. fraction of octene } w_{OCT} = \frac{38}{100} = 0.38$$

$$\text{wt. fraction of ethylene } w_{ET} = 1 - w_{OCT} = 1 - 0.38 = 0.62$$

$$\text{Molar fraction of octene} = x_{OCT}$$

$$x_{OCT} = \frac{\frac{w_{OCT}}{M_{OCT}}}{\frac{w_{OCT}}{M_{OCT}} + \frac{w_{ET}}{M_{ET}}} = \frac{\frac{0.38}{112.216}}{\frac{0.38}{112.216} + \frac{0.62}{28.054}} = 0.13287. \tag{10}$$

$$\text{Molar fraction of ethylene} = x_{ET} = 1 - x_{OCT} = 1 - 0.13287 = 0.86713$$

Average molecular weight of repeating unit:

$$M_{ET-OCT} = x_{ET}M_{ET} + x_{OCT}M_{OCT} = 0.86713 \cdot 28.054 + 0.13287 \cdot 112.216 = 39.2364 \text{ g/mol}$$

$$\text{Polymerization degree} = P_n = \frac{M_{nEOC}}{M_{ET-OCT}} = \frac{61469}{39.2364} = 1567$$

Charlesby–Pinner equation:

$$s + \sqrt{s} = \frac{p_0}{q_0} + \frac{1}{q_0 P_n D}$$

$$\text{In plot } s + \sqrt{s} \text{ vs. } \frac{1}{D}\text{: intercept} = \frac{p_0}{q_0},\ \text{slope} = \frac{1}{q_0 P_n}$$

$$\text{In case of EOC-38 : intercept} = 0.1752,\ \text{slope} = 35.93$$

$$\text{then } \frac{p_0}{q_0} = 0.1752 \text{ and } \frac{1}{q_0 P_n} = 35.93$$

$$q_0 = \frac{1}{\text{slope} \cdot P_n} = \frac{1}{35.93 \cdot 1567} = 0.00001777$$

$$\text{then } p_0 = q_0 \cdot \text{intercept} = q_0 \cdot \frac{p_0}{q_0} = 0.00001777 \cdot 0.1752 = 0.000003113.$$

Calculation of G parameters according to Charlesby-Pinner equation (see Table 2):

$$s + \sqrt{s} = \frac{G(S)}{2G(X)} + \frac{4.82 \times 10^6}{G(X)M_nD}$$

$$\text{then } \frac{G(S)}{2G(X)} = \frac{p_0}{q_0}$$

$$\frac{G(X)}{G(S)} = \frac{1}{2\frac{p_0}{q_0}} = \frac{1}{2 \cdot 0.1752} = 2.8539$$

$$\text{slope} = \frac{4.82 \times 10^6}{G(X)M_n}$$

$$G(X) = \frac{4.82 \times 10^6}{\text{slope} \cdot M_n} = \frac{4.82 \times 10^6}{35.93 \cdot 61469} = 2.1824$$

$$\text{intercept} = \frac{G(S)}{2G(X)}$$

$$G(S) = 2 \cdot G(X) \cdot \text{intercept} = 2 \cdot 2.1824 \cdot 0.1752 = 0.7647$$

Table 2 Calculation of Charlesby–Pinner parameters

wt% of octene	wt. fraction of octene	wt. fraction of ethylene	Molar fraction of octene	Molar fraction of ethylene	$M_{\text{ET-OCT}}$	M_n	P_n
0	0.00	1.00	0.00000	1.00000	28.0540	41,104	1465
17	0.17	0.83	0.04871	0.95129	32.1536	48,564	1510
30	0.30	0.70	0.09677	0.90323	36.1987	55,456	1532
38	0.38	0.62	0.13287	0.86713	39.2364	61,469	1567
Slope	p_0/q_0	q_0	p_0	$G(X)/G(S)$	$G(X)$	$G(S)$	
34.27	0.6137	1.992E−05	1.222E−05	0.8147	3.4218	4.1999	
35.15	0.4330	1.884E−05	8.156E−06	1.1547	2.8236	2.4453	
35.37	0.2812	1.845E−05	5.189E−06	1.7781	2.4573	1.3820	
35.93	0.1752	1.777E−05	3.113E−06	2.8539	2.1824	0.7647	

Appendix 3

During my study of the literature concerning ethylene–octene copolymers, I found many interesting papers, but quite a large number of them did not have correct values of octene content or melt flow index. This could be caused by the fact that the manufacturer at the present time does not list comonomer content in their materials data sheets. These numbers appeared briefly on the DuPont-Dow Elastomers' web page in the year 2002, but then, this information disappeared. Fortunately, I have this table, and I would like to share it with the wider scientific community (see Table 3, columns 1–4). In addition, I have added comonomer content in mol% in column 5 and ethylene/octene molar ratio (see column 6). The molar fraction of octene was calculated according to Eq. 10.

Table 3 Engage® product chart

Engage® grade	Comonomer content ^{13}C NMR/FTIR (wt%)	Density ASTM D-792 (g/cm^3)	Melt index ASTM D-1238 190 °C, 2.16 kg (dg/min)	Calculated comonomer content (mol %)	Ethylene/octene molar ratio
8842	45	0.857	1.0	16.98	4.9
8180	42	0.863	0.5	15.33	5.5
8130	42	0.864	13.0	15.33	5.5
8400/8407	40	0.870	30.0	14.29	6.0
8150/8157	39	0.868	0.5	13.78	6.3
8100/8107	38	0.870	1.0	13.29	6.5
8200/8207	38	0.870	5.0	13.29	6.5
8452	35	0.875	3.0	11.86	7.4
8411	33	0.880	18.0	10.96	8.1
8401	31	0.885	30.0	10.10	8.9
8003	30	0.885	1.0	9.68	9.3
8440	23	0.897	1.6	6.95	13.4
8402	22	0.902	30.0	6.59	14.2
8490	21	0.902	7.5	6.23	15.0
8480	20	0.902	1.0	5.88	16.0
8450	20	0.902	3.0	5.88	16.0
8550	20	0.902	4.3	5.88	16.0
8540	17	0.908	1.0	4.87	19.5
8445	16	0.910	3.5	4.55	21.0
8403	16	0.913	30.0	4.55	21.0

DuPont Dow Elastomers. http://www.dupont-dow.com. Rev. 2, July 2002 (columns 1–4). Columns 5 and 6 were calculated by the author of this paper

References

1. Chum PS, Kruper WJ, Guest MJ (2000) Materials properties derived from INSITE metallocene catalysts. Adv Mater 12(23):1759–1767
2. Chum PS, Kao CI, Knight GW (1995) Structure-property relationships in polyolefins made by constrained geometry catalyst technology. Plast Eng 51(6):21–23
3. Alamo RG, Viers BD, Mandelkern L (1993) Phase-structure of random ethylene copolymers—a study of counit content and molecular-weight as independent variables. Macromolecules 26(21):5740–5747
4. Bensason S, Minick J, Moet A, Chum S, Hiltner A, Baer E (1996) Classification of homogeneous ethylene-octene copolymers based on comonomer content. J Polym Sci Pt B Polym Phys 34(7):1301–1315
5. Wood-Adams PM, Dealy JM, deGroot AW, Redwine OD (2000) Effect of molecular structure on the linear viscoelastic behavior of polyethylene. Macromolecules 33(20):7489–7499
6. Li JQ, Peng J, Qiao JL, Jin DB, Wei GS (2002) Effect of gamma irradiation on ethylene-octene copolymers. Radiat Phys Chem 63(3–6):501–504
7. Casey P, Chen HY, Poon B, Bensason S, Menning B, Liu LZ et al (2008) Polyolefin based cross-linked elastic fiber: a technical review of DOW XLA (TM) elastic fiber technology. Polym Rev 48(2):302–316
8. Abe S, Yamaguchi M (2001) Study on the foaming of crosslinked polyethylene. J Appl Polym Sci 79(12):2146–2155
9. Vachon C, Gendron R (2003) Effect of gamma-irradiation on the foaming behavior of ethylene-co-octene polymers. Radiat Phys Chem 66(6):415–425
10. Chen HY, Chum SP, Hiltner A, Baer E (2001) Comparison of semicrystalline ethylene-styrene and ethylene-octene copolymers based on comonomer content. J Polym Sci Pt B Polym Phys. 39(14):1578–1593
11. Kale LT, Plumley TA, Patel RM, Jain P, Tappi (1995) Structure-property relationships of ethylene/1-octene and ethylene/1-butene copolymers made using insite technology. 1995 Polymers, laminations & coatings conference, books 1 and 2. Tappi, Atlanta, pp 423–433
12. Eynde SV, Mathot VBF, Koch MHJ, Reynaers H (2000) Thermal behaviour and morphology of homogeneous ethylene-1-octene copolymers with high comonomer contents. Polymer. 41(13):4889–4900
13. Molloy BM, Hyslop DK, Parent JS (2014) Comparative analysis of delayed-onset peroxide crosslinking formulations. Polym Eng Sci 54(11):2645–2653
14. Nicolas J, Ressia JA, Valles EM, Merino JC, Pastor JM (2009) Characterization of metallocene ethylene-1-octene copolymers with high comonomer content cross-linked by dicumyl peroxide or beta-radiation. J Appl Polym Sci 112(5):2691–2700
15. de Melo RP, Aguiar VDO, Marques MDFV (2015) Silane crosslinked polyethylene from different commercial PE's: influence of comonomer, catalyst type and evaluation of HLPB as crosslinking coagent. Mater Res Ibero Am J 18(2):313–319
16. Sirisinha K, Chuaythong P (2014) Reprocessable silane-crosslinked polyethylene: property and utilization as toughness enhancer for high-density polyethylene. J Mater Sci 49(14):5182–5189
17. Sirisinha K, Boonkongkaew M (2013) Improved silane grafting of high-density polyethylene in the melt by using a binary initiator and the properties of silane-crosslinked products. J Polym Res 20(4):9
18. Singh P, Kumar R, Singh R, Roychowdhury A, Das D (2015) The influence of cross-linking and clustering upon the nanohole free volume of the SHI and gamma-radiation induced polymeric material. Appl Surf Sci 328:482–490
19. Karabelli D, Lepretre JC, Dumas L, Rouif S, Portinha D, Fleury E et al (2015) Crosslinking of poly(vinylene fluoride) separators by gamma-irradiation for electrochemical high power charge applications. Electrochim Acta 169:32–36
20. Ghosal S, Mukhopadhyay M, Ray R, Tarafdar S (2014) Competitive scission and cross linking in a solid polymer electrolyte exposed to gamma irradiation: simulation by a fractal model. Phys A 400:139–150
21. Zimek Z, Przybytniak G, Nowicki A, Mirkowski K, Roman K (2014) Optimization of electron beam crosslinking for cables. Radiat Phys Chem 94:161–165

22. Ng HM, Bee ST, Ratnam CT, Sin LT, Phang YY, Tee TT et al (2014) Effectiveness of trimethylopropane trimethacrylate for the electron-beam-irradiation-induced cross-linking of polylactic acid. Nucl Instrum Methods Phys Res Sect B Beam Interact Mater Atoms 319:62–70
23. Zhu SF, Shi MW, Zhu MF (2013) Effects of electron-beam irradiation crosslinking on PA6 fibers. Fiber Polym 14(4):525–529
24. Makuuchi K, Cheng S (2012) Radiation processing of polymer materials and its industrial applications. Wiley, Hoboken, New Jersey, USA
25. Charlesby A, Pinner SH (1959) Analysis of the solubility behaviour of irradiated polyethylene and other polymers. Proc R Soc Lond Ser A 249(1258):367–386
26. Dubey KA, Chaudhari CV, Rao R, Bhardwaj YK, Goel NK, Sabharwal S (2010) Radiation processing and characterization of poly(vinyl alcohol) nano-composites, part 1: nano-particulate filler tuned crosslinking behavior. J Appl Polym Sci 118(6):3490–3498
27. Mondal M, Gohs U, Wagenknecht U, Heinrich G (2013) Efficiency of high energy electrons to produce polypropylene/natural rubber-based thermoplastic elastomer. Polym Eng Sci 53(8):1696–1705
28. Turgis JD, Coqueret X (1999) Electron beam sensitivity of butyl acrylate copolymers: effects of composition on reactivity. Macromol Chem Phys 200(3):652–660
29. Mussatti FG, Macosko CW (1973) Rheology of network forming systems. Polym Eng Sci 13(3):236–240
30. Colby RH, Fetters LJ, Graessley WW (1987) Melt viscosity molecular-weight relationship for linear-polymers. Macromolecules 20(9):2226–2237
31. Sirisinha K, Chimdist S (2008) Silane-crosslinked ethylene-octene copolymer blends: thermal aging and crystallization study. J Appl Polym Sci 109(4):2522–2528
32. Liu ZY, Chen SJ, Zhang J (2011) Photodegradation of ethylene-octene copolymers with different octene contents. Polym Degrad Stab 96(11):1961–1972
33. Svoboda P, Poongavalappil S, Theravalappil R, Svobodova D, Mokrejs P (2013) Effect of octene content on peroxide crosslinking of ethylene-octene copolymers. Polym Int 62(2):184–189
34. Gupta J, Nunes C, Vyas S, Jonnalagadda S (2011) Prediction of solubility parameters and miscibility of pharmaceutical compounds by molecular dynamics simulations. J Phys Chem B 115(9):2014–2023